

*Inorg. Chem. Res.*, Vol. 2, No. 2, , December 2019

DOI: 10.22036/icr.2019.200120.1053

## Synthesis, Characterization and Catalytic Study of a Novel Binuclear *Paddle-wheel* Palladium(II) Complex in the Mizoroki-Heck Reaction

V. Amani<sup>a,\*</sup>, A.S. Delbari<sup>b</sup>, A. Akbari<sup>c</sup>, M.R. Poor Heravi<sup>d</sup> and M. Amini<sup>e,\*</sup>

<sup>a</sup>Department of Chemistry, Farhangian University, Tehran, Iran

<sup>b</sup>Young Researchers and Elite Club, Islamshahr Branch, Islamic Azad University, Islamshahr, Iran

<sup>c</sup>Cellular and Molecular Research Center, Research Institute for Cellular and Molecular Medicine, Urmia University of Medical Sciences, Urmia, Iran

<sup>d</sup>Payame Noor University, Department of Chemistry, 19395-4697 Tehran, Iran

<sup>e</sup>Department of Chemistry, Faculty of Science, University of Maragheh, Maragheh, Iran

(Received 1 September 2019, Accepted 4 September 2019)

A new binuclear *paddle-wheel* palladium(II) complex of  $[\text{Pd}_2(\mu\text{-mtzt})_4]\text{dmgH}_2$  (1) has been prepared by the treatment of  $\text{PdCl}_2$  in acetonitrile with mixture of 1-methyl-1H-1,2,3,4-tetrazole-5-thiol (Hmtzt) and dimethylglyoxime ( $\text{dmgH}_2$ ) in methanol. Resulted complex was characterized by elemental analysis (CHNS), IR, UV-Vis absorption,  $^1\text{H}$  NMR spectroscopy and its structure was determined with single-crystal X-ray diffraction. Single crystal analysis reveals that this complex has binuclear structure in a *paddle-wheel* fashion with Pd-Pd distances of 2.808(2) Å. Also, in this binuclear complex, each palladium(II) ion has a slightly distorted square-pyramidal coordination geometry with the two nitrogen and two sulfur atoms in equatorial positions from four bridges  $\text{mtzt}^-$  ligands and the second palladium subunit in axial position. Catalytic potentiality of complex 1 is also exhibited in the Mizoroki-Heck coupling reactions between a range of aryl halides and olefins. The catalyst shows very much efficient reactivity in the Mizoroki-Heck reactions giving high yield of the coupling products.

**Keywords:** Binuclear palladium(II) complex, Crystal structure, 1-Methyl-1H-1,2,3,4-tetrazole-5-thiol, Mizoroki-Heck reaction

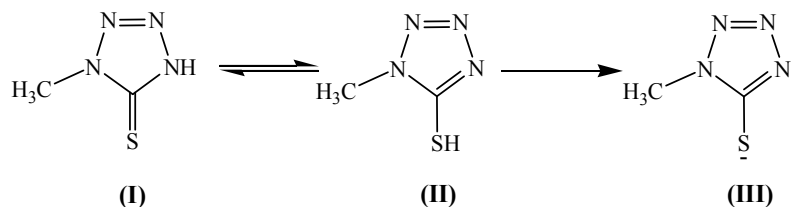
### INTRODUCTION

The heterocyclic thioamide compound of 1-methyl-1,2,3,4-tetrazole-5-thiol, with  $-\text{NH}-\text{C}(=\text{S})- \leftrightarrow -\text{N}=\text{C}(-\text{SH})-$  functional moiety, has thione and thiol tautomerism forms in the solution state, while this compound in the solid state is in thione form (Scheme 1) [1,2]. This compound in the anionic form,  $\text{mtzt}^-$ , is a good multidentate ligand with four potential donor atoms (one S atom from thiol group and three N atoms from tetrazole ring), and can be coordinated to main metals and transition metals (in

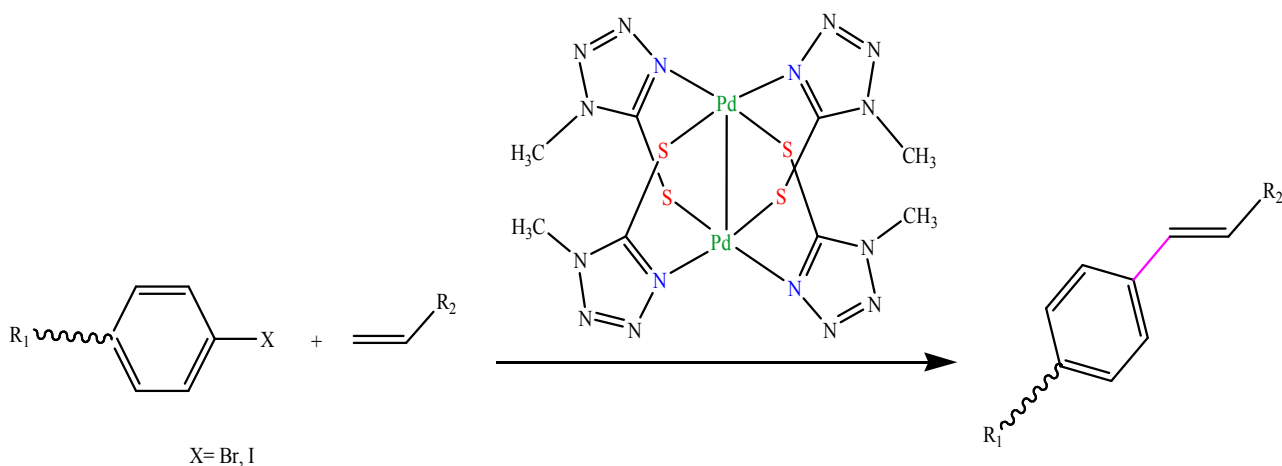
deferent oxidation state). Coordination may lead to the formation of the mononuclear, binuclear, 1D coordination polymers and 2D coordination polymers with several interesting different structures [2-14].

Variety of catalytic systems constructed from palladium complexes has been intensively developed for the C-C bond formation *via* the Mizoroki-Heck coupling reaction of aryl halides with a wide range of olefinic substrates, due to their availability, low cost and environmental benignity [15-22]. Clearly, the development of air and thermally stable catalysts with high activity and broad substrate tolerance is needed to allow reactions to be carried out under mild reaction conditions, then to broader industrial use of the reaction.

\*Corresponding authors. E-mail: [v.amani@cfu.ac.ir](mailto:v.amani@cfu.ac.ir); [mamini@maragheh.ac.ir](mailto:mamini@maragheh.ac.ir)



Scheme 1. (I) Thione tautomer, (II) thiol tautomer and (III) anionic form of Hmtzt



Scheme 2. Mizoroki-Heck coupling reactions in the presence of binuclear palladium(II) complex,  $[\text{Pd}_2(\mu\text{-mtzt})_4]\text{dmgH}_2$

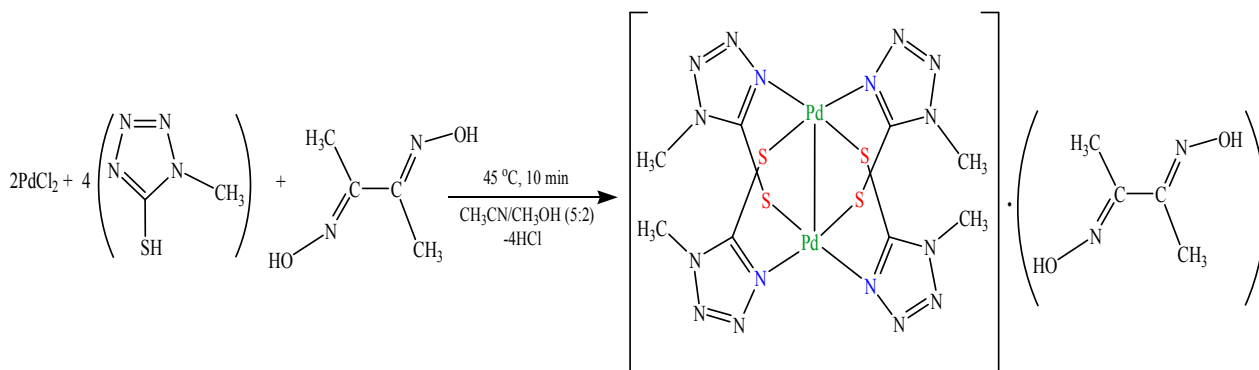
Recently some of us reported preparation and characterization of a binuclear *paddle-wheel* complex of  $[\text{Pd}_2(\mu\text{-mtzt})_4]$  [4], which was synthesized by the reaction of 1-methyl-1,2,3,4-tetrazole-5-thiol and  $\text{PdCl}_2$  in mixture of acetonitrile/methanol. In this paper, a new binuclear *paddle-wheel* complex of  $[\text{Pd}_2(\mu\text{-mtzt})_4]\text{dmgH}_2$  (1) has been prepared by the reaction of  $\text{PdCl}_2$  salt in acetonitrile with the mixture of 1-methyl-1H-1,2,3,4-tetrazole-5-thiol and dimethylglyoxime ligands in methanol. This complex was fully characterized and its structure was analyzed by single-crystal X-ray diffraction method. Moreover catalytic activity of the mentioned complex in the Mizoroki-Heck coupling reactions between a range of aryl halides and olefins under mild reaction condition is explored. Noticeably, an overall investigation of the effective parameters on the Mizoroki-Heck reaction such as solvent, bases reaction time and temperature is described

(Scheme 2).

## EXPRIMENTAL

### Materials and Physical Methods

1-Methyl-1H-1,2,3,4-tetrazole-5-thiol (Hmtzt) and dimethylglyoxime ( $\text{dmgH}_2$ ) were purchased from Aldrich, and used as received.  $\text{PdCl}_2$  and all solvents were purchased from Merck and used without further purification. Elemental (C, H, N, S) analysis was performed using an Elementar Analysensystem GmbH VarioEL.  $^1\text{H}$  NMR spectrum was taken on a Bruker FT-NMR 300 MHz spectrometer using dimethyl sulfoxide- $\text{d}_6$  as solvent. UV-Vis absorption spectrum was taken on a Perkin Elmer Precisely PTP-1 Peltier System using a 1 cm path length cell in DMSO at room temperature. Infrared spectrum ( $4000\text{-}250\text{ cm}^{-1}$ ) was taken on a Shimadzu-470 spectrometer in CsI pellets.



Scheme 3. The preparation method for complex 1

### Synthesis of $[\text{Pd}_2(\mu\text{-mtzt})_4]\text{dmgH}_2$ (1)

A suspension of  $\text{PdCl}_2$  (0.15 g, 0.84 mmol) in 100 ml acetonitrile was stirred and warmed to  $75\text{ }^\circ\text{C}$ , to give an orange solution. Then, a mixture of 1-methyl-1H-1,2,3,4-tetrazole-5-thiol (0.10 g, 0.84 mmol) and dimethylglyoxime (0.10 g, 0.84 mmol) in 20 ml methanol was added to the solution and the mixture was stirred at  $45\text{ }^\circ\text{C}$  for 10 min. The resulting orange solution was filtered. Orange prismatic crystals are obtained at room temperature after five days (yield 0.26 g, 78.4%, m. p.  $> 270\text{ }^\circ\text{C}$ ). IR (CsI,  $\text{cm}^{-1}$ ): 3411br, 2951w, 1557m, 1470m, 1385s, 1308s, 1249s, 1178s, 1086s, 984s, 914s, 838m, 714s, 616m, 514m, 501m, 348m, 256m. UV-Vis:  $\lambda_{\text{max}}$  (DMSO, nm), 264, 402.  $^1\text{H}$  NMR (DMSO- $d_6$ , ppm): 2.18 (s, 6H), 3.84 (s, 12H) and 5.54 (s, 2H). Anal. Calcd. for  $\text{C}_{12}\text{H}_{20}\text{N}_{18}\text{O}_2\text{Pd}_2\text{S}_4$  (%): C, 18.25; H, 2.53; N, 31.92; S, 16.21. Found: C, 18.10; H, 2.51; N, 31.76; S, 16.11.

### General Procedures for the Heck Reaction

An appropriate amount of aryl halide (1.0 mmol), olefin (1.1 mmol) and  $\text{K}_2\text{CO}_3$  (1.1 mmol) were added to a solution of 1 in (1:1) mixture of DMF/ $\text{H}_2\text{O}$  (2 ml). The mixture was heated to  $100\text{ }^\circ\text{C}$  with stirring for a specified period of time. After cooling of the reaction mixture to room temperature, HCl (1 M, 6 ml) was added and the coupling product was extracted with ethyl acetate ( $2 \times 15$  ml). After separation of the organic layer from the aqueous solution, it was washed with water ( $2 \times 10$  ml), dried over  $\text{CaCl}_2$ , and evaporated to dryness under reduced pressure to afford the desired product.

### X-ray Structure Analysis

The X-ray diffraction measurements for single crystal of  $[\text{Pd}_2(\mu\text{-mtzt})_4]\text{dmgH}_2$  (1) was made on a Bruker APEX II CCD area-detector diffractometer at 298 K using graphite mono-chromated Mo  $\text{K}\alpha$  radiation ( $\lambda = 0.71073\text{ \AA}$ ). The structure of 1 was solved by SHELX-97 and absorption correction was applied using the SADABS program [23]. Data collection, cell refinement, and data reduction were performed by applying APEX II, SAINT, SHELXTL and PLATON program packages [23-25]. The ORTEP and crystal packing diagram for title complex were drawn with the Mercury 2.4 program software [26].

## RESULTS AND DISCUSSION

### Synthesis of Compound $[\text{Pd}_2(\mu\text{-mtzt})_4]\text{dmgH}_2$ (1)

Complex 1 was prepared from the reaction mixture of one equivalent of 1-methyl-1H-1,2,3,4-tetrazole-5-thiol and one equivalent of dimethylglyoxime in methanol with one equivalent of  $\text{PdCl}_2$  in acetonitrile, at  $45\text{ }^\circ\text{C}$  for 10 min. Suitable crystals of title complex were obtained for X-ray diffraction measurement by slow evaporation of the resulted orange solution at room temperature. The synthetic route of title complex is shown in Scheme 3.

### Spectroscopic Characterization of $[\text{Pd}_2(\mu\text{-mtzt})_4]\text{dmgH}_2$ (1)

The IR absorption bands for title complex are listed in the experimental section. The infrared spectrum for this complex shows a broad absorption band at around

3411  $\text{cm}^{-1}$  and a weak absorption band at 2951  $\text{cm}^{-1}$ , which are assigned to the O-H and C-H stretching bands respectively, for the free dimethylglyoxime compound [27]. Infrared spectrum of free 1-methyl-1H-1,2,3,4-tetrazole-5-thiol ligand has been reported previously [28]. In the IR spectrum of this free ligand, the two medium absorption bands appeared at 2681 and 2652  $\text{cm}^{-1}$  can be assigned to the N-H stretching vibrations in the thione form [28]. In IR spectrum of **1** these medium absorption bands disappeared, that indicates the 1-methyl-1H-1,2,3,4-tetrazole-5-thiol ligand has been deprotonated and Pd-S and Pd-N bonds have been formed [28]. The multiple absorption bands appeared in the range 1557-1249  $\text{cm}^{-1}$  have been assigned to C-C, C-N, N-N, C=N and N=N stretching vibrations. Also, the multiple medium to strong absorption bands appeared in the range 1178-501  $\text{cm}^{-1}$  have been assigned to the C-S stretching and C-S, C-C, N-O, N-N and C-N deformation vibrations in the tetrazole ring and free dimethylglyoxime compound [2-4,27,28]. Furthermore, the strong absorption band appeared at 984  $\text{cm}^{-1}$  has been assigned to the N-O stretching vibration of free dimethylglyoxime compound [27]. Far infrared spectrum for title complex was recorded between 400 and 250  $\text{cm}^{-1}$ . The medium absorption bands appeared at 348 and 256  $\text{cm}^{-1}$  have been assigned to the Pd-S and Pd-N, stretching vibrations, respectively [4].

The  $^1\text{H}$  NMR spectrum for title complex was prepared in dimethyl sulfoxide- $d_6$  solution at room temperature and the results are listed in the experimental section. The  $^1\text{H}$  NMR spectrum of this complex exhibited two singlet bands at 2.18 and 3.84 ppm for the methyl group of the uncoordinated  $\text{dmgH}_2$  and coordinated  $\text{mtzt}^-$  compounds, respectively. Furthermore, the peak observed at 5.54 ppm in the  $^1\text{H}$  NMR spectrum of **1** has been assigned to =N-OH of uncoordinated  $\text{dmgH}_2$  compound. Absence of the signal of the -NH or -SH protons (12.82 ppm) in the thione or thiol forms of the free Hmtzt ligand in the  $^1\text{H}$  NMR spectrum of **1** shows that the ligand is deprotonated and confirms that Pd-N and Pd-S bonds are formed [2,3].

The UV-Vis absorption spectrum of **1** in dimethyl sulfoxide solution at room temperature exhibited a strong broad absorption band at around 264 nm which can be assigned to the ligand-centered  $\pi \rightarrow \pi^*$  and  $n \rightarrow \pi^*$  transitions. In addition, the weak broad absorption band

appeared at around 402 nm is assigned to the metal-metal-to ligand charge transfer (MMLCT) transitions [28].

### Description of the Molecular Structures of $[\text{Pd}_2(\mu\text{-mtzt})_4]\text{dmgH}_2$ (**1**)

Crystallographic data for this complex are given in Table 1 and selected bond lengths and angles are presented in Table 2. This complex crystallizes in the monoclinic crystal system with  $C2/c$  space group. The molecular structure of the binuclear title complex together with the atomic labeling scheme is shown in Fig. 1. As shown in this figure, the asymmetric unit of **1** contains one half of independent  $[\text{Pd}_2(\mu\text{-mtzt})_4]$  complex and half of uncoordinated  $\text{dmgH}_2$  compound. As depicted in Fig. 1, the structure of complex  $[\text{Pd}_2(\mu\text{-mtzt})_4]$  consists of binuclear *paddle-wheel* unit and each palladium(II) cation has a distorted square-pyramidal coordination geometry with the two nitrogen and two sulfur atoms in equatorial positions from four bridges  $\text{mtzt}^-$  ligands and the second palladium subunit in axial position. In this binuclear complex, the Pd1-Pd1<sup>i</sup> (i is -x+1, -y+1, -z+1) distance is 2.808(2) Å, which is similar to  $[\text{Pd}_2(\mu\text{-mtzt})_4].2\text{CH}_3\text{CN}$ , 2.8021(11) Å [4], but is longer than in complex of  $[\text{Pd}_2(\mu\text{-Clhp})_4]$  (2.567(2) Å), [29] and complex of  $[\text{Pd}_2(\mu\text{-Mepyth})_4].2\text{HCCl}_3$  (2.677 Å), [30] (where Clhp is 6-chloro-2-hydroxypyridinate and Mepyth is 4-methylpyridine-2-thiolate). The Pd-N bond lengths are 2.055(10) and 2.083(11) Å and Pd-S bond lengths are 2.292(4) and 2.302(3) Å. In this binuclear *paddle-wheel* complex of  $[\text{Pd}_2(\mu\text{-mtzt})_4]$ , the five-membered Pd-N-C-S-Pd rings are roughly planar and nearly perpendicular to each other. The N1<sup>i</sup>-Pd1-N5<sup>i</sup>, N5<sup>i</sup>-Pd1-S1, N1<sup>i</sup>-Pd1-S2 and S1-Pd1-S2 (i is -x+1, -y+1, -z+1) angles are 87.5(7), 90.8(3), 89.5(3) and 90.72(15)°, respectively. The Pd-N and Pd-S bond lengths and the S-Pd-S, S-Pd-N and N-Pd-N bond angles (Table 2) are in good agreement with the corresponding values in  $[\text{Pd}_2(\mu\text{-mtzt})_4].2\text{CH}_3\text{CN}$  [4].

Crystal packing diagram for  $[\text{Pd}_2(\mu\text{-mtzt})_4]\text{dmgH}_2$  (**1**) are shown in Figs. 2 and 3. In the crystal structure of this complex, there are two short and strong intermolecular S...S and Pd...S contacts which links all complexes into a one-dimensional chain polymer along the crystallographic b axis (Fig. 2). The distances of S1...S2<sup>i</sup>, S2...S2<sup>i</sup> and Pd1...S2<sup>i</sup> (i is 3/2-x, -1/2+y, 3/2-z) are 3.414(6), 3.532(2)

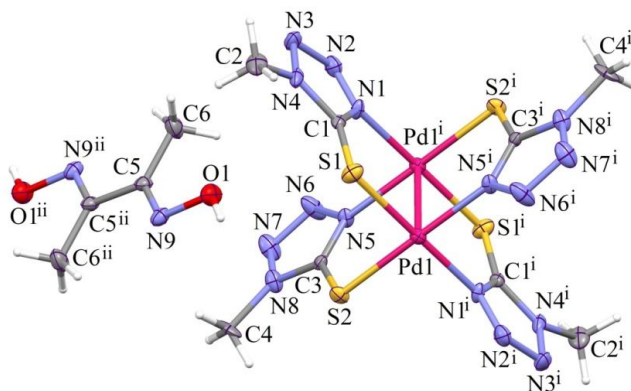
**Table 1.** Crystallographic and Structure Refinement Data for 1

Formula	C <sub>12</sub> H <sub>20</sub> N <sub>18</sub> O <sub>2</sub> Pd <sub>2</sub> S <sub>4</sub>
Formula weight	789.58
Temperature (K)	298(2)
Wavelength $\lambda$ (Å)	0.71073
Crystal system	Monoclinic
Space Group	C2/c
Crystal size (mm <sup>3</sup> )	0.45 × 0.40 × 0.32
<i>a</i> (Å)	26.305(9)
<i>b</i> (Å)	6.6097(17)
<i>c</i> (Å)	17.001(7)
$\beta$ (°)	116.39(3)
Volume (Å <sup>3</sup> )	2647.9(16)
Z	4
Density (calc.) (g cm <sup>-3</sup> )	1.981
$\theta$ ranges for data collection	1.73-26.99
F(000)	1560
Absorption coefficient mm <sup>-1</sup>	1.725
	-33 ≤ <i>h</i> ≤ 33
Index ranges	-8 ≤ <i>k</i> ≤ 7
	-21 ≤ <i>l</i> ≤ 21
Data collected	11607
Unique data ( <i>R</i> <sub>int</sub> )	2896, 0.0985
Parameters, restraints	175, 0
Final <i>R</i> <sub>1</sub> , <i>wR</i> <sub>2</sub> (Obs. data)	0.0313, 0.0815
Final <i>R</i> <sub>1</sub> , <i>wR</i> <sub>2</sub> (All data)	0.0450, 0.0945
Goodness of fit on <i>F</i> <sup>2</sup> (S)	1.002
Largest diff peak and hole (e Å <sup>-3</sup> )	1.006, -1.005
CCDC No.	1581109

**Table 2.** Bond Distances (Å) and Bond Angles (°) for 1

Pd1-N5 <sup>i</sup>	2.055(10)	N5 <sup>i</sup> -Pd1-S1	90.8(3)
Pd1-N1 <sup>i</sup>	2.083(11)	N1 <sup>i</sup> -Pd1-S1	179.1(4)
Pd1-S1	2.292(4)	N5 <sup>i</sup> -Pd1-S2	177.8(3)
Pd1-S2	2.302(3)	N1 <sup>i</sup> -Pd1-S2	89.5(3)
Pd1-Pd1 <sup>i</sup>	2.808(2)	S1-Pd1-S2	90.72(15)
N5 <sup>i</sup> -Pd1-N1 <sup>i</sup>	89.0(4)		

Symmetry code: (i) -x+1, -y+1, -z+1.

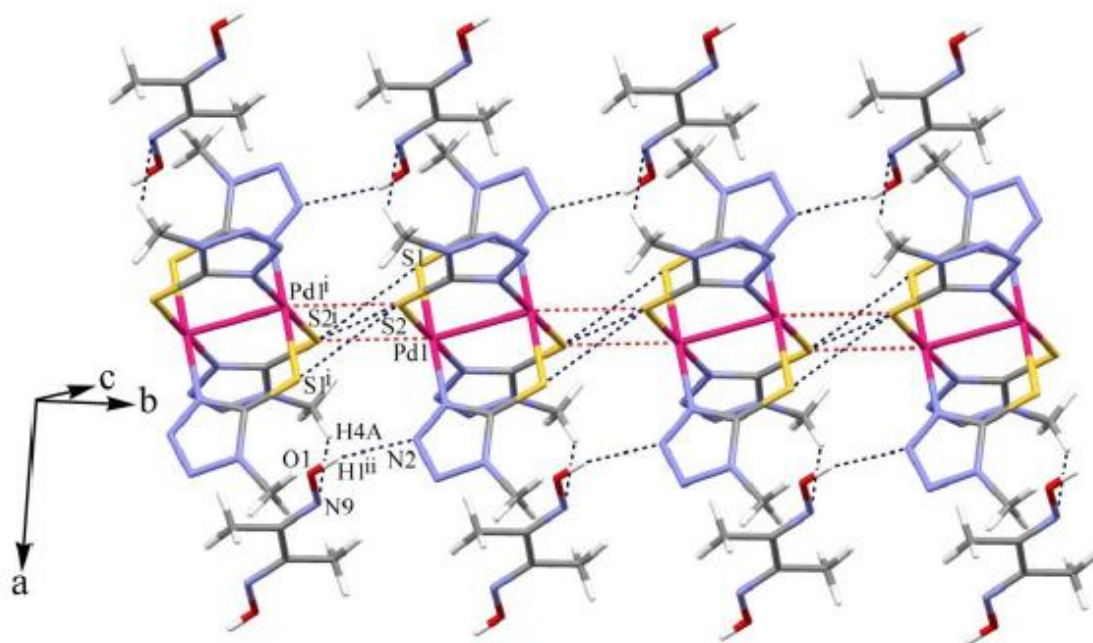
**Fig. 1.** The labeled diagram of  $[\text{Pd}_2(\mu\text{-mtzt})_4]\text{dmgH}_2$  (1). Thermal ellipsoids are at the 30% probability level. Symmetry codes: (i) -x+1, -y+1, -z+1 and (ii) -x+3/2, -y+3/2, -z+1.

and 3.146(4) Å, respectively, which are shorter than the sum of the van der Waals radii of the two S atoms and one Pd and one S atom (3.7 Å for S...S and 4.04 Å for Pd...S) [31,32]. It is notable that in this complex, there are intra- and intermolecular C-H...N and O-H...N hydrogen bonds (Table 3) in the crystal packing. These S...S and Pd...S interactions and also intra- and intermolecular C-H...N and O-H...N hydrogen bonds causing on the stabilization of this complex in the crystal packing (Figs. 2 and 3).

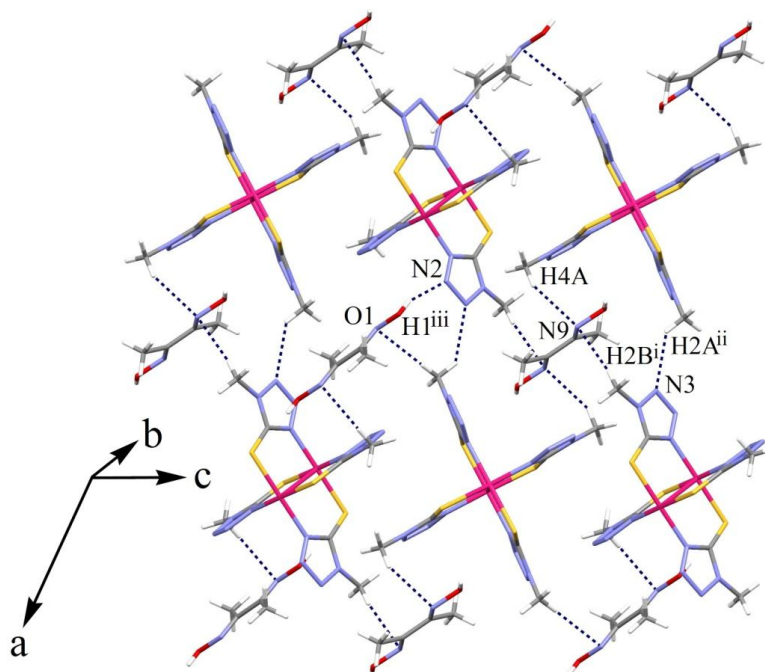
### Catalytic Effects

Catalytic studying began with an effort to optimize reaction conditions for the Mizoroki-Heck reaction. 4-Bromoacetophenone and n-butyl acrylate as model substrates were used in order to optimize the reaction conditions (Table 4). In the absence of catalyst as a

blank experiment (entry 1), trace amount of coupling product were observed, which indicated that the presence of a catalyst is crucial. Further screening with using PdCl<sub>2</sub> as a catalyst giving moderate yield which is comparatively lower than that obtained with 1 (entries 2, 6). To find the best solvent for the coupling reaction of model substrates, various solvents such as H<sub>2</sub>O, DMSO, DMF, DMF/H<sub>2</sub>O, ethanol and toluene were screened (entries 3-8). The polar solvent DMF and DMSO gave high yield, however a less-polar solvent like toluene was demonstrated to be inefficient. Protic green solvents H<sub>2</sub>O and ethanol afforded coupling product in low yields. The reaction in (1:1) mixture of DMF/H<sub>2</sub>O showed an almost quantitative yield (entry 6). We further investigated the catalytic efficiency by



**Fig. 2.** Polymer organization in  $[\text{Pd}_2(\mu\text{-mtzt})_4]\text{dmgH}_2$  (1) due to  $\text{S}\cdots\text{S}$  and  $\text{Pd}\cdots\text{S}$  interactions and  $\text{O-H}\cdots\text{N}$  and  $\text{C-H}\cdots\text{N}$  hydrogen bonds. Symmetry codes: (i)  $1-x, 2-y, 1-z$  and (ii)  $x, 1+y, z$ .



**Fig. 3.** Crystal packing diagram for  $[\text{Pd}_2(\mu\text{-mtzt})_4]\text{dmgH}_2$  (1). The intra- and intermolecular  $\text{C-H}\cdots\text{N}$  and  $\text{O-H}\cdots\text{N}$  hydrogen bonds are shown as dashed lines. Symmetry codes: (i)  $3/2-x, -1/2+y, 3/2-z$ ; (ii)  $3/2-x, 1/2+y, 3/2-z$  and (iii)  $x, 1+y, z$ .

**Table 3.** Hydrogen Bond Geometry for 1 in Crystal Packing

D-H...A	D-H (Å)	H...A (Å)	D...A (Å)	D-H...A (°)	Symmetry code
O1-H1...N2	0.82	2.390	3.172(18)	160	x, 1+y,z
C2-H2A...N3	0.96	2.600	3.37(2)	137	3/2-x, 1/2+y, 3/2-z
C4-H4A...N9	0.96	2.600	3.408(19)	142	-
C2-H2B...N9	0.96	2.650	3.60(2)	168	3/2-x, -1/2+y, 3/2-z

varying the amount of the catalyst with the other conditions kept the same as above (entries 9, 10). By continuously increasing the catalyst amount from 0.001 mmol to 0.002 mmol, a significant increase in the yield was observed. Further increase of the catalyst amount to 0.003 mmol showed no significant effect on the product yield (entry 10). Among the bases  $K_2CO_3$  was found to be a superior over  $Na_2CO_3$  and  $Na_3PO_4$ , whereas the other bases  $NH_3$ ,  $NaOAc$ ,  $KOH$  gave lower yield (entries 11-15). As indicated in Table 4, a strong decrease of yield is obtained with reducing the reaction temperature from 100 °C to room temperature (entries 16-18). Also the reaction times were varied to get the quantitative yield of product and a significant improvement in the product yield was observed at 6 h (entries 19, 20).

The optimized reaction conditions were then extended to a range of different aryl halides and olefins to examine the substrate scope of the reaction and the results are summarized in Table 5. Aryl halides containing electron-withdrawing groups gave excellent yields compared to aryl halides containing electron-donating groups (entries 3-5 and 8-11). For example, coupling of 4-COCH<sub>3</sub> substituted aryl iodide with n-butyl acrylate gave 97% yield when compared to 4-CH<sub>3</sub>O substituted aryl iodides, which gave 94% of yield (entries 3 and 5). Furthermore, aryl iodides substituted with CH<sub>3</sub>O group at ortho position were less reactive to the coupling reaction than the *para* derivative due to steric hindrance of the *ortho* substituents on the aryl iodides (entries 4-7). Studies are also extended to less reactive aryl bromides which furnished moderate yield because of the

strong C-Br bond compared to C-I bond (entries 12 and 13).

To show the quality and performance of the present catalytic system in comparison with recently reported systems, we compared the results of the Mizoroki-Heck coupling reaction of 4-bromoacetophenone and n-butyl acrylate in the presence of other catalysts. As shown in Table 6, our catalytic system is preferred to some of the previously reported catalysts in terms of reaction conditions and yield. In contrast to similar, previously reported systems, the catalytic system presented in this paper does not suffer from the harsh reaction conditions, such as using long reaction time (entry 2), a large amount of catalyst (entry 3), and high reaction temperature (entry 2).

## CONCLUSIONS

In conclusion, we have synthesized a new binuclear *paddle-wheel* palladium(II) complex,  $[Pd_2(\mu\text{-mtzt})_4]dmgH_2$ , by the treatment of  $PdCl_2$  with mixture of 1-methyl-1H-1,2,3,4-tetrazole-5-thiol and dimethylglyoxime. The studies described herein indicate that the  $[Pd_2(\mu\text{-mtzt})_4]dmgH_2$  complex catalyzes the Mizoroki-Heck coupling reactions between a range of aryl halides and olefins under mild reaction condition in an excellent yield.

## ACKNOWLEDGEMENTS

The authors are grateful to the Farhangian University, Islamic Azad University (Islamshahr Branch), and University of Maragheh for financial support.

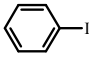
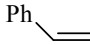
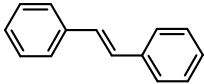
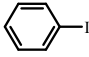
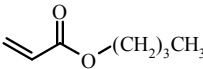
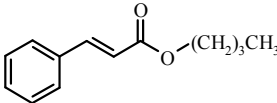
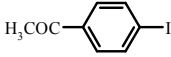
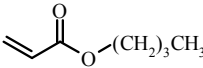
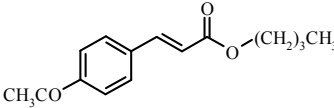
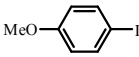
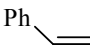
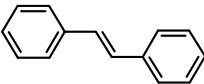
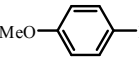
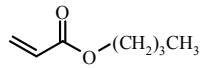
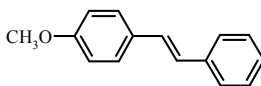
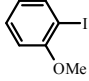
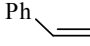
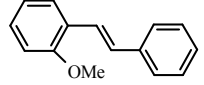
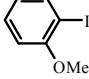
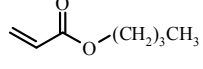
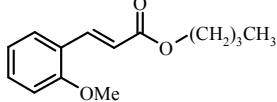
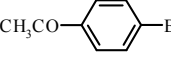
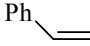
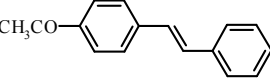
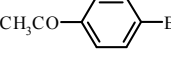
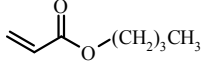
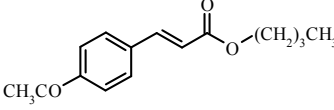
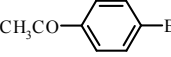
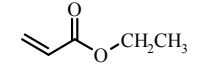
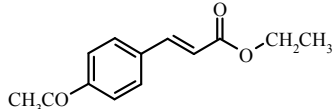

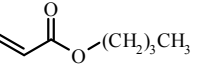
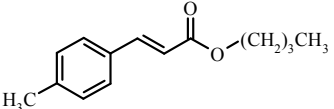
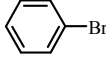
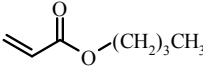
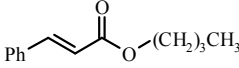
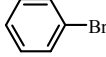
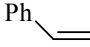
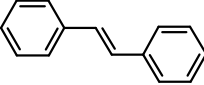


**Table 4.** The Effect of Various Conditions on the Heck Reaction in the Presence of 1<sup>a</sup>

Entry	Amount of catalyst	catalyst	Base	Solvent	Temperature (°C)	Time (h)	Yield (%) <sup>b</sup>
1	0.002	-	K <sub>2</sub> CO <sub>3</sub>	DMF/H <sub>2</sub> O	100	6	-
2	0.002	PdCl <sub>2</sub>	K <sub>2</sub> CO <sub>3</sub>	DMF/H <sub>2</sub> O	100	6	38
3	0.002	1	K <sub>2</sub> CO <sub>3</sub>	H <sub>2</sub> O	100	6	26
4	0.002	1	K <sub>2</sub> CO <sub>3</sub>	DMSO	100	6	65
5	0.002	1	K <sub>2</sub> CO <sub>3</sub>	DMF	100	6	88
6	0.002	1	K <sub>2</sub> CO <sub>3</sub>	DMF/H <sub>2</sub> O	100	6	96
7	0.002	1	K <sub>2</sub> CO <sub>3</sub>	ethanol	100	6	21
8	0.002	1	K <sub>2</sub> CO <sub>3</sub>	toluene	100	6	8
9	0.001	1	K <sub>2</sub> CO <sub>3</sub>	DMF/H <sub>2</sub> O	100	6	57
10	0.003	1	K <sub>2</sub> CO <sub>3</sub>	DMF/H <sub>2</sub> O	100	6	95
11	0.002	1	Na <sub>2</sub> CO <sub>3</sub>	DMF/H <sub>2</sub> O	100	6	79
12	0.002	1	Na <sub>3</sub> PO <sub>4</sub>	DMF/H <sub>2</sub> O	100	6	66
13	0.002	1	NH <sub>3</sub>	DMF/H <sub>2</sub> O	100	6	11
14	0.002	1	NaOAc	DMF/H <sub>2</sub> O	100	6	34
15	0.002	1	KOH	DMF/H <sub>2</sub> O	100	6	25
16	0.002	1	K <sub>2</sub> CO <sub>3</sub>	DMF/H <sub>2</sub> O	r.t.	6	5
17	0.002	1	K <sub>2</sub> CO <sub>3</sub>	DMF/H <sub>2</sub> O	50	6	29
18	0.002	1	K <sub>2</sub> CO <sub>3</sub>	DMF/H <sub>2</sub> O	70	6	64
19	0.002	1	K <sub>2</sub> CO <sub>3</sub>	DMF/H <sub>2</sub> O	100	2	34
20	0.002	1	K <sub>2</sub> CO <sub>3</sub>	DMF/H <sub>2</sub> O	100	4	58

<sup>a</sup>Reaction conditions: 1.0 mmol of aryl halide, 1.2 mmol of olfins, 2 mmol of base, 2 ml solvent;<sup>b</sup>Isolated yield.

**Table 5.** Heck Reaction between Aryl halides and Olefins in the Presence of 1 as a Catalyst<sup>a</sup>

Entry	Ar-X	Olefins	Products	Yield (%) <sup>b</sup>	TON <sup>c</sup>
1				97	485
2				97	485
3				97	485
4				93	465
5				94	470
6				79	395
7				83	415
8				95	475
9				96	480
10				96	480
11				82	410
12				61	305
13				56	280

<sup>a</sup>Reaction conditions: 1.0 mmol of aryl halide, 1.2 mmol of olefins, 2 mmol of K<sub>2</sub>CO<sub>3</sub>, 2 ml DMF/H<sub>2</sub>O, 100 °C, 6 h;<sup>b</sup>Isolated yield. <sup>c</sup>TON: mol products/mol catalyst.

**Table 6.** Recently Reported Catalytic Systems in the Mizoroki-Heck Coupling Reaction by Various Palladium Complexes

Entry	Catalyst	Condition	Yield (%)	Ref.
1	1	0.002 mmol of catalyst, H <sub>2</sub> O/DMF, 100 °C, 6 h	96	Present work
2	Pd(oxazine) <sub>2</sub>	0.002 mmol of catalyst, DMAc, 120 °C, 8 h	79	[22]
3	Pd(OAc) <sub>2</sub>	0.005 mmol of catalyst, H <sub>2</sub> O/DMSO, 80 °C, 4 h	83	[20]

## REFERENCES

- [1] R.C. Olivares, O.J. Sandoval, S.H. Ortega, M. Sanchez, R.A. Toscano, I. Haiduc, *Heteroat. Chem.* 6 (1995) 89.
- [2] M. Taheriha, M. Ghadermazi, V. Amani, *J. Mol. Struct.* 1107 (2016) 57.
- [3] M.S. Majdolashrafi, A. Raissi Shabari, V. Amani, *Phosphorus Sulfur Silicon Relat. Elem.* 192 (2017) 1188.
- [4] S. Seyfi, R. Alizadeh, M. Darvish Ganji, V. Amani, *Spectrochimica Acta Part A*: 190 (2018) 298.
- [5] A.G. Zavaglia, I.D. Reva, L. Frija, M.L. Cristiano, R. Fausto, *J. Mol. Struct.* 786 (2006) 182.
- [6] H. Nöth, W. Beck, K. Burger, *Eur. J. Inorg. Chem.* (1998) 93.
- [7] S. Chen, *Z. Kristallogr. NCS* 227 (2012) 213.
- [8] E.S. Lang, M. Dahmer, U. Abram, *Acta Crystallogr. C* 55 (1999) 854.
- [9] Y.L. Wanga, Q. Shi, W.H. Bi, X. Li, R. Cao, *Z. Anorg. Allg. Chem.* 632 (2006) 167.
- [10] S. Ibáñez, D.N. Vrečo, F. Estevan, P. Hirva, M. Sanaú, M.A. Úbeda, *Dalton Trans.* 43 (2014) 2961.
- [11] Y. Yang, J. Gong, W. Zhang, H. Zhang, L. Zhang, Y. Liu, H. Huang, H. Hu, Z. Kang, *RSC. Adv.* 2 (2012) 6414.
- [12] M. Imran, A. Mix, B. Neumann, H.G. StammLer, U. Monkowius, P. Bleckenwegner, N.W. Mitzel, *Dalton Trans.* 43 (2014) 14737.
- [13] U. Abram, J.R. Dilworth, *Z. Anorg. Allg. Chem.* 625 (1999) 609.
- [14] M. Imran, A. Mix, B. Neumann, H.G. StammLer, U. Monkowius, P. Bleckenwegner, N.W. Mitzel, *Dalton Trans.* 44 (2015) 924.
- [15] D. Dallinger, C.O. Kappe, *Chem. Rev.* 107 (2007) 2563.
- [16] R.A. Sheldon, *Green Chem.* 7 (2005) 267.
- [17] F. Diederich, P.J. Stang, *Metal-Catalyzed Cross-Coupling Reactions*, Wiley-VCH, Weinheim, Germany, 1998.
- [18] M. Amini, D.B. Heydarloo, M. Rahimi, M.G. Kim, S. Gautam, K.H. Chae, *Mater. Res. Bull.* 83 (2016) 179.
- [19] L.S. Søbjerg, D. Gauthier, A.T. Lindhardt, M. Bunge, K. Finster, R.L. Meyer, T. Skrydstrup, *Green Chem.* 11 (2009) 2041.
- [20] M. Amini, M. Bagherzadeh, Z. Moradi-Shoeili, D.M. Boghaei, *RSC Adv.* 2 (2012) 12091.
- [21] S.M.S. Hussain, M.B. Ibrahim, A. Fazal, R. Suleiman, M. Fettouhi, B.E. Ali, *Polyhedron* 70 (2014) 39.
- [22] M. Bagherzadeh, M. Amini, A. Ellern, L.K. Woo, *Inorg. Chim. Acta* 383 (2012) 46.
- [23] G.M. Sheldrick, *SADABS*. Madison, WI, USA: Bruker AXS, 1998.
- [24] Bruker SMART and SAINT. Madison, WI, USA: Bruker AXS Inc., 1998.

- [25] G.M. Sheldrick. Acta Crystallogr. A64 (2008) 112.
- [26] Mercury 141. Copyright Cambridge Crystallographic Data Center. Cambridge, 2001-2005.
- [27] S.S.A. Abidi, Y. Azim, A.K. Gupta, C.P. Pradeep, J. Mol. Struct. 1150 (2017) 103.
- [28] M.S. Majdolashrafi, A. Raissi Shabari, V. Amani, Phosphorus Sulfur Silicon Relat. Elem. 193 (2018) 415.
- [29] W. Clegg, C.D. Garner, M.H. Al-Samman, Inorg. Chem. 21 (1982) 1897.
- [30] K. Umakoshi, A. Ichimura, I. Kinoshita, S. Ooi, Inorg. Chem. 29 (1990) 4005.
- [31] A. Abedi, V. Amani, R. Boča, L. Dlháň, H.R. Khavasi, N. Safari, Inorg. Chim. Acta 395 (2013) 58.
- [32] S. Alvarez, Dalton Trans. 42 (2013) 8617.